A three-scale approach to the numerical simulation of metallic bonding for MEMS packaging

Aldo Ghisi [a], Stefano Mariani [a], Alberto Corigliano [a,*], Giorgio Allegato [b], Laura Oggioni [b]

[a] Politecnico di Milano, Dipartimento di Ingegneria Civile e Ambientale, piazza L. da Vinci 32, 20133 Milano, Italy
[b] STMicroelectronics, AMS – MEMS Technology Development, via C. Olivetti 2, 20864 Agrate Brianza, Italy

Article history:
Received 27 June 2014
Accepted 8 July 2014
Available online 10 August 2014

1. Introduction

The sealing of microsystems can become an issue, because of the strong requirements imposed by the drive to miniaturization. In order to shrink the overall dimensions of packaged devices, metallic rings with decreasing planar width can be used to insulate the cavity where, for example, inertial accelerometers or gyroscopes are placed at low vacuum pressures. One can wonder how far it is possible to stretch down the dimensions of the metallic ring, and whether features of the geometry of the rings themselves can affect the effectiveness of the sealing. Moreover, while for wafer-to-wafer bonding the thermo-compression process seems particularly appealing, it is difficult to rationally interpret the link between the final bonding strength and the variables controlling the bonding process, such as the pressure and temperature inside the chamber, and the roughness of the metallic surfaces entering into contact. In these cases it has been recognised [1] that the surface energy adhesion, the surface roughness and the material deformation play key roles for a good bonding.

In a wafer-to-wafer thermo-compression process two silicon wafers, each one with its own pattern of metallic rings, are pushed together while the temperature is increased during a thermal cycle. A re-crystallization process then occurs inside and between the two metallic rings, leading to a metallurgical bonding [2–4]. There have been several studies focused on the characterisation of the thermo-compression bonding [5–7], and nowadays refined studies on grain growth can be pursued (see, e.g. [8]), but there are many issues still to be clarified. Progressing on the research line initiated in [9], we adopt here a simplified approach in the analysis, and consider the final material in the sealing layer as a continuum, mechanically stressed by the chamber pressure. Overall variables, like the pressure and temperature, but also the misalignment of the two wafers getting into contact and the roughness of the metallic layers, are then linked to the mechanical behaviour of the sealing through a top-down, multi-scale (three-scale) approach. To this aim we consider in sequence, from the largest to the smallest level: at the macro-scale, the response of the whole silicon wafer(s) under the external compressive force; at the meso-scale, the effects of stress concentrations arising from the metallic ring geometry at the contact interface for a typical silicon die; at the micro-scale, a representative volume of the metallic ring accounting for the local surface roughness. The information flows uni-directionally from macro-scale to micro-scale, and allows to evaluate the quality of the bonding in terms of area entering into contact under the truly local pressure. This approach can single out possible bonding issues due to inhomogeneities in the local pressure, due to different choices in the in-plane or out-of-plane ring layouts.

In the next Section 2 the hypotheses adopted for the modelling at each scale are described, while in Section 3 the numerical procedure is applied to a typical geometry used for MEMS metallic bonding. The validity of the approach is qualitatively checked against shear test experimental results in Section 4. Final remarks are proposed in Section 5.

* Corresponding author.
E-mail addresses: aldo.ghisi@polimi.it (A. Ghisi), stefano.mariani@polimi.it (S. Mariani), alberto.corigliano@polimi.it (A. Corigliano), giorgio.allegato@st.com (G. Allegato), laura.oggioni@st.com (L. Oggioni).

2. Description of the proposed approach

The rationale behind our approach initiated in [9], and already adopted to study the reliability of inertial MEMS sensors exposed to shocks, see [10,11], is a decoupling of the phenomena occurring at the different length-scales. In this specific analysis of thermo-mechanical metallic bonding, three scales are singled out: a macroscopic one, at the silicon wafer level; a mesoscopic one, at the single die level; and a microscopic one, at the polycrystal level. Within a top-down, uncoupled approach, the information flows from the larger to the smaller scale, as we implicitly assume that the response at the lower scale does not affect the one at the upper scales. For sake of simplicity, we adopt a purely mechanical point of view, neglecting the full thermo-mechanical coupling, but considering the mechanical properties of the materials involved in the bonding process as temperature-dependent ones: hence, those relevant to the temperature at which the bonding occurs have been adopted in the analyses.

The macro-scale model allows for the two silicon wafers entering into contact because of a compressive force given by the hydraulic jack in the bonding chamber. During the production phase, this operation is actually carried out in a bonding chamber where temperature and pressure are strictly controlled; this is accounted for in the simulation by modifying accordingly the mechanical properties of the materials (e.g. Young's modulus, yield strength). The wafers are modelled as homogeneous thin shells, taking into account the small ratio between their thickness and radius.

The actual contact area, represented for each single die by the metallic bonding ring, is instead modelled with a spring placed at the centre of mass of each ring. The spring stiffness, which is a nonlinear function of the relative out-of-plane displacement between the two shells, aims to represent the overall behaviour of two metallic rings attached to the die and cap wafers, when pushed against each other by the out-of-plane force. A simplified, piecewise linear spring response is adopted as shown in Fig. 1. As the interaction between the two wafers is null till contact, the force is zero up to a relative displacement amounting to the initial gap g; at increasing displacement, the elastic behaviour of the ring comes into play to define the overall elastic stiffness $K = \frac{EA}{\ell}$, where E is its Young's modulus, A the contact area and ℓ the total bonding ring thickness. Beyond the elastic regime, a perfectly plastic response of the ring is assumed according to a von Mises yield criterion [12], with force transmitted constant and equal to F_y. The mechanical properties of silicon and metallic ring adopted in the analysis are the following: the elastic modulus along each axis of orthotropy of silicon is 130.1 GPa, the Poisson's ratio is 0.28, and the shear modulus is 80 GPa; the metallic ring is assumed as isotropic and elastic perfectly plastic, whose Young's modulus is 75 GPa, Poisson's ratio is 0.34, and yield strength σ_y is 50 MPa.

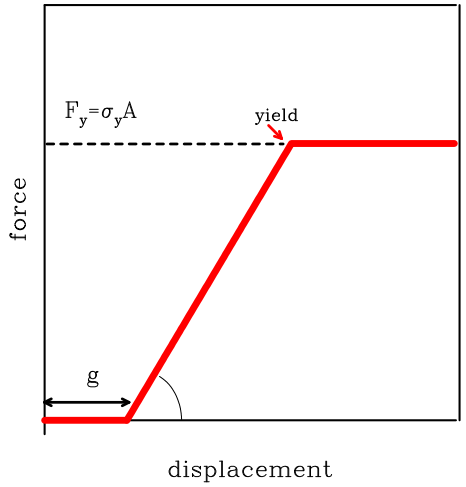

Fig. 1. Assumed nonlinear spring behaviour.

The main output of the macro-scale analysis consists in the force acting on the single spring, i.e. in the global force acting on each die ring.

This information is next transferred to the meso-scale as a pressure acting over the silicon wafers, obtained as the spring force divided by the die area. To account for the (quasi) periodic solution relevant to one die, at this length-scale displacements are restrained along the lateral surfaces of die and cap in the local direction normal to the surfaces themselves. The actual geometry of the metallic ring is described at this length-scale, so that the effects of the stress concentrations in regions of the contact area can be studied, see Fig. 2. Accordingly, the ring is not lumped in a spring but instead modelled as a three-dimensional solid. At this level, we focus on the local out-of-plane pressure acting on the ring surfaces getting into contact. It is therefore assumed that such pressure is not influenced much by the imperfections of the interface between the upper and the lower rings. The relevant uncertainties of the aforementioned imperfections, basically linked to the microstructure of the polycrystalline films, will be later accounted for at the micro-scale. At the micro-scale, a representative volume of the metallic ring, with in-plane dimensions on the order of 1 μm × 1 μm, is modelled. We describe the roughness properties of the contact surface through an algorithm used in [13], and based on the work of Hu and Tonder [14]: each surface of one ring is obtained as a realisation of a stochastic process with a Gaussian probability density function, whose standard deviation is defined via the root mean square (rms) value. The local out-of-plane pressure obtained with the meso-scale analysis is now handled to drive the contact-induced deformation of the ring volume. The displacements along the lateral surfaces of the representative volume are restrained in the local normal direction, whereas top and bottom surfaces are acted upon by the local pressure measured at the meso-scale. The resulting contact area, defined as the percentage of the whole in-plane area of the two rings entering into contact when the asperities of the upper and lower surface are plastically deformed, is eventually adopted to measure the quality of the sealing: the higher the contact area, the closer the mechanical properties of the bonding to the reference metallic ring ones.

3. Results and discussion

In this Section we provide results relevant to the definition of the strength properties of the metallic ring, as obtained via the

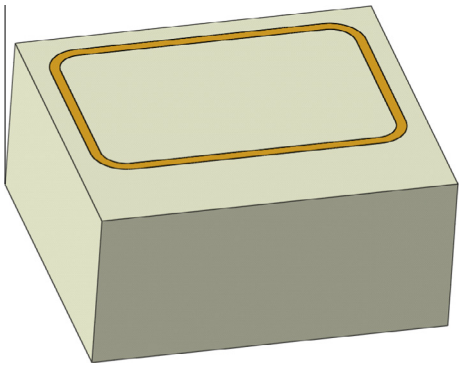

Fig. 2. Meso-scale. Overview of the metallic ring and die (cap has been removed for clarity).

proposed top-down approach. Such results will be then qualitatively validated in Section 4 against the outcomes of a shear test carried out on a representative device. Main features of the solution at the sealing ring level are discussed in what follows at the meso- and micro-scales only. At the macro-scale, as already said, the whole wafers (or a part of them, allowing for possible macroscopic and mesoscopic, i.e. at die level, symmetries) are modelled as thin or moderately thick shells. The interaction between the two plates, and the resulting stress state, is only governed by the nonlinear properties of the spring modelling the metallic ring(s) of each die. Accordingly, the space discretization has been designed so as to resolve the stress state in the silicon wafers. To provide a figure of the computational burden tied to this macro-scale analysis, it suffices to say that one quarter (due to symmetries) of each wafer has been discretized with around 65,000 shell finite elements.

Under the action of the out-of-plane compressive force provided by the hydraulic jack, the local stress distribution in silicon appears as depicted in Fig. 4, with a quasi-periodic pattern due to the relevant geometry of the rings here considered.

At the meso-scale, a die of dimensions $1580 \times 1390 \times 1454$ μm has been considered. The metallic ring, whose geometry is as reported in Fig. 5, has a width of around 50 μm, and a total thickness of 4 μm. To discretize its bulk, and attain a rather accurate evaluation of the stress field inside it, 500,000 tetrahedral finite elements have been adopted.

As detailed in Section 2, the axial force in the spring modelling the metallic ring is adopted at this scale as a compressive force acting over the die and cap. The two rings in between are hence pushed against each other, and the pressure in the direction perpendicular to the substrate (once again, in the out-of-plane direction) is monitored to assess the efficiency of sealing.

Stress concentrations across the width of the ring and along the whole longitudinal axis of the ring itself may appear, as reported in Fig. 5. Such concentrations are primarily due to the different widths of the two rings attached to die and cap, purposely adopted to cope with possible misalignments of the two wafers during the thermo-compression process. Besides this effect, additional fluctuations of the pressure field can be due to the local geometry of the ring. Accordingly, close to corners stress enhancement can be accompanied by a levelling off of the stress field in neighbouring regions, which are likely to provide a reduced strength of the sealed ring and, therefore, a premature failure under the external actions.

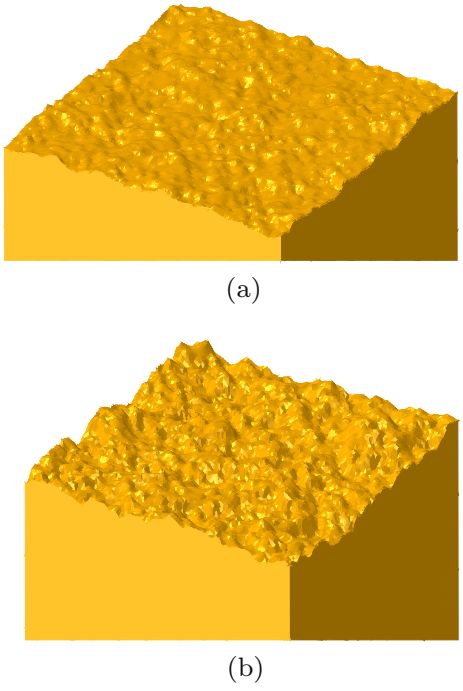

Fig. 3. Micro-scale. Examples of digital models with (a) low surface roughness, rms = 10 nm, and (b) high surface roughness, rms = 50 nm.

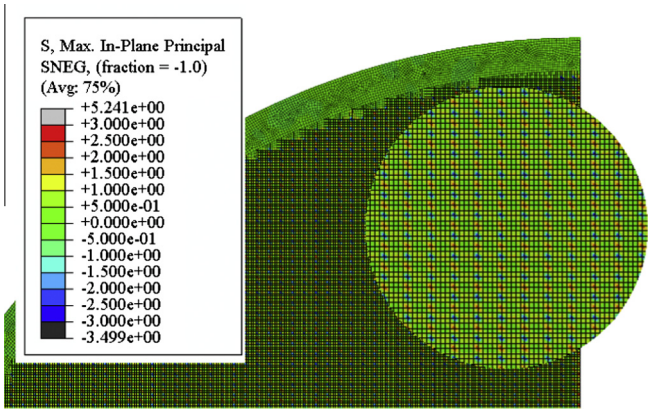

Fig. 4. Macro-scale analysis. Local maximum principal stress distribution (in MPa) in a portion of silicon wafer.

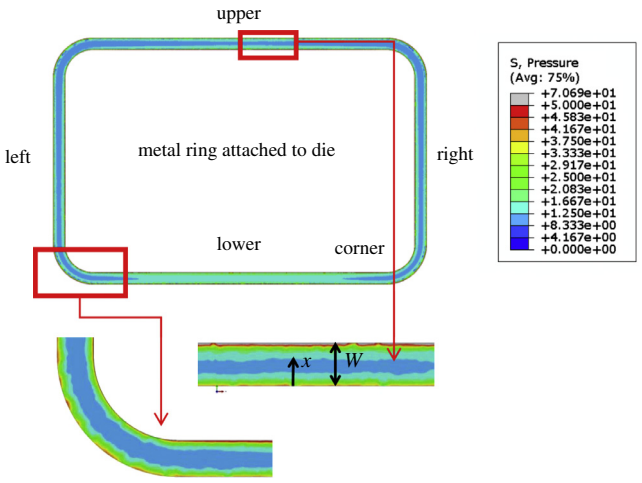

Fig. 5. Meso-scale analysis. Sketch of the pressure field (in MPa) over the contact surface between the two metallic rings, and notation concerning the regions where the stress field is monitored.

We specifically focus the attention to the five regions, or locations identified in Fig. 5. For the considered geometry, while the solution in terms of the pressure p acting on the contact surface is symmetric about the vertical axis of symmetry of the geometry, some scattering between the upper and lower regions turns out to be related to minor differences in die and cap geometries to accommodate the pads. This is further reported in Fig. 6, which shows a non-dimensional graph of p across the width of the contact surface in all the regions checked, p_{max} being the maximum value of p all over the ring. These plots show quantitatively what discussed here above: stress enhancement occurs along the lateral borders of the sealing surface, due to the interaction of the two corners of the lower ring (here attached to the die) with the flat surface of the other, wider ring (here attached to the cap); in a central part of the bonding ring (amounting to about 60–70% of its total width) the pressure gets reduced, to a value of about 25% of the peak one. This is expected to be the weakest link of the whole bonding, where possible failure processes can be triggered.

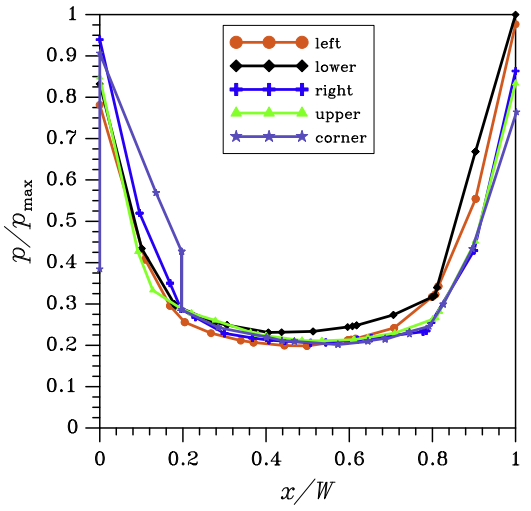

Fig. 6. Meso-scale analysis. Evolution of the pressure field acting along the contact surfaces across the ring width, at the five locations identified in Fig. 5.

Down to this length-scale, stochastic effects have not been considered. At the micro-scale, representative volumes of the two rings are modelled with a side length of 1 μm. As already discussed in Section 2, roughness is parametrically described by the rms value. At this scale, to accurately resolve the stress state in the bulk of the film, around 200,000 tetrahedral finite elements have been adopted in the analysis.

By progressively increasing the local, out-of-plane compressive force measured at the meso-scale, the asperity of the two surfaces get flattened and the micro-contact area increases. Needless to say, the higher the rms value (the higher the roughness) the higher the compressive force required to attain a target value of the contact area/representative volume surface ratio. The red spots, progressively spreading all over the surface in Fig. 7, represent the aforementioned micro-contact effective area. The relevant evolution is mainly governed by the yielding of the metallic material inside the two ring volumes modelled; due to the geometry of the asperity, as shown in Fig. 3, such yielding occurs initially close to the contact surface and, only when the micro-contact area fraction approaches values higher than 80–90%, spreads inside the bulk of the ring.

The value of the fraction micro-contact/total areas can eventually be adopted as a measure of the effectiveness of sealing.

4. Results validation: shear test

To validate the proposed multi-scale approach to define the properties of the sealing ring, we report here results of a shear test (adapted from the MIL-STD-883E-2019 standard [15]) carried out on a single device, as shown in the schematic of Fig. 8. Due to the set-up of the test, the stress field in the metal ring can be claimed to be actually shear-dominated; to feature a pure shear stress field in the whole ring, the cap would need to be appropriately constrained to avoid a rocking-type displacement. Accordingly, in this Section we provide only a qualitative assessment of the results through the comparison of experimental data with numerical estimations of the sealing response to the lateral load.

The effect of the load is to induce first an elastic response, followed by a plateau due to the perfectly plastic behaviour of the ring, see the exemplary numerical results shown in Fig. 9. An analytical estimate of the ultimate load is given by the in-plane area A of the ring amplifying the effective shear strength T_y^* of the ring itself, as induced by the thermo-mechanical bonding process. The value of T_y^* is defined as the weighted average one all over the meso-scopic contact surface, according to $T_y^* = \frac{1}{A}\int_A \alpha T_y \, dA$, where T_y is the strength of the perfect bulk metal, and α is the local, space varying ratio between the micro-contact area and the total surface area, as obtained with the micro-scopic analysis of the multi-scale approach. From Fig. 9 it appears that numerical simulation relevant to the low roughness case is consistent with the experimental results. When the surface roughness is low, in fact, the applied local pressure on the ring turns out to be sufficient to involve a very large contact area; this is confirmed by the value of the estimated shear strength, which is reasonably close to the experimental value (affected by a $\pm 5\%$ uncertainty indicated by the cyan shaded area in Fig. 9). When the high rms case is instead considered, the contact area decreases dramatically for the applied pressure values, and the estimated shear strength leads to a very weak bond.

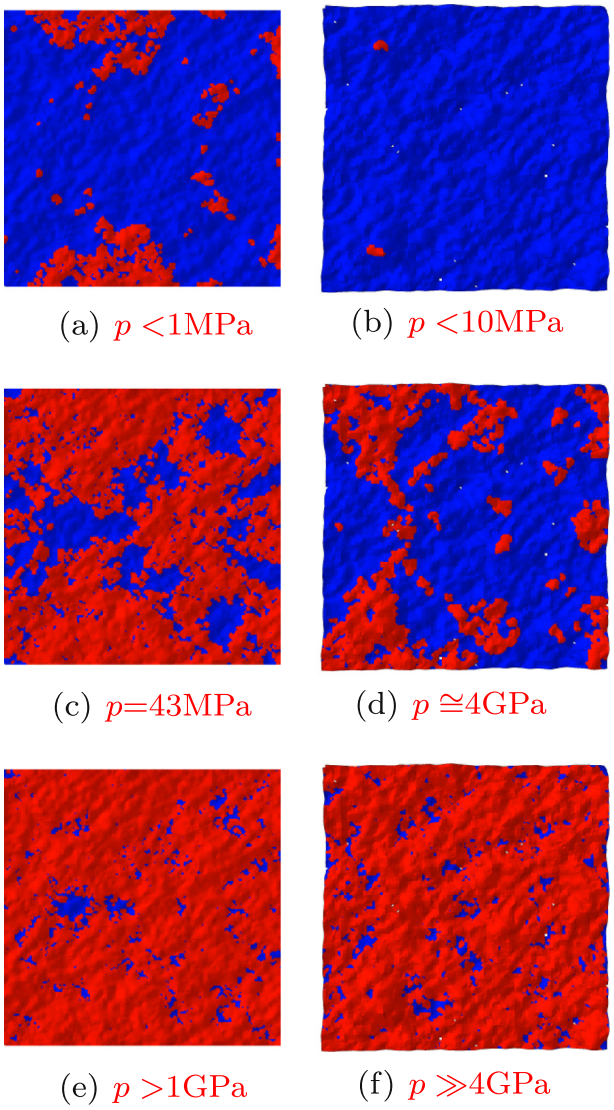

Fig. 7. Micro-scale analysis. Micro-contact area at increasing out-of-plane pressure level from top to bottom. Left column rms = 10 nm, right column rms = 50 nm.

5. Conclusions

A top-down, uncoupled, multi-scale numerical approach has been proposed to estimate the quality of the sealing in a wafer-to-wafer thermo-compression bonding.

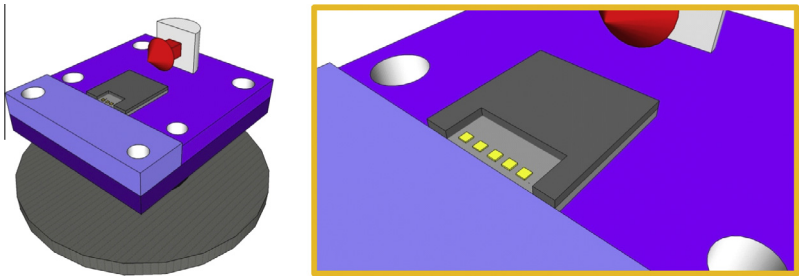

Fig. 8. Schematic of the shear test used for validation.

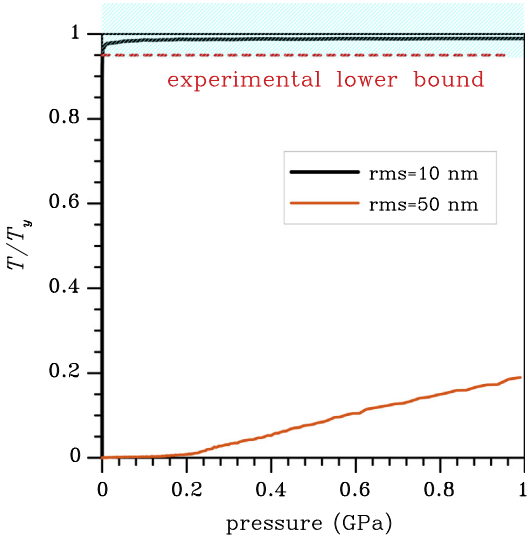

Fig. 9. Shear test. Comparison of numerical and experimental shear forces.

The transition from the wafer length-scale to the local scale on the metallic ring level, is implemented through three models, each one describing a target region of the wafers or of the rings. The proposed procedure allows to estimate the percentage of contact area as a function of the mean surface roughness and of the applied pressure. This result is a first step to understand how the local geometry of the metallic rings may affect the quality of the bonding; it would also allow to study the role of mis-alignments of the rings attached to the die and of other geometrical defects.

This method will be completed in the future with the full description of the thermo-mechanical coupling effects, and with a statistical evaluation of the overall contribution of surface roughness through, e.g., Monte Carlo simulations.

Acknowledgement

Part of this work has been carried out in the framework of Eniac Joint Undertaking Project Lab4MEMS, Grant No. 325622.

References

[1] Gui C, Elwenspoek M, Tas N, Gardeniers J. The effect of surface roughness on direct wafer bonding. J Appl Phys 1999;85:7448–54.
[2] Greer J, Hosson JD. Plasticity in small-sized metallic systems: intrinsic versus extrinsic size effect. Prog Mater Sci 2011;56:654–725.
[3] Chen X, Ngan A. Specimen size and grain effects on tensile strength of Ag microwires. Scripta Mater 2011;64:717–20.
[4] Espinosa H, Prorok B. Size effects on the mechanical behavior of gold thin films. J Mater Sci 2003;38:4125–8.
[5] Tsau C. Fabrication and characterization of wafer–level gold thermocompression bonding. Ph.D. thesis, Massachusetts Institute of Technology; 2003.
[6] Farrens S. Wafer-bonding technologies and strategies for 3D ICs. In: Tan CS, Gutman RJ, Reif LR, editors. Wafer level 3-D ICs process technology, integrated circuits and systems; 2008. p. 49–85.
[7] Tsau C, Spearing SM, Schmidt M. Characterization of wafer-level thermocompression bonds. J Microelectromech Syst 2004;13:963–71.
[8] Kim D-U, Cha P-R, Kim S, Kim W, Cho J, Han H-N. Effect of micro-elasticity on grain growth and texture evolution: a phase field grain growth evolution. Comput Mater Sci 2012;56:56–68.
[9] Ghisi A. Corigliano A, Mariani S, Allegato G. A multi-scale approach to wafer metallic bonding in MEMS. In: 14th International conference on thermal, mechanical and multi-physics simulation and experiments in microelectronics and microsystems, EuroSimE 2013, Wrocław, Poland, April 14–17; 2013. p. 6529905.
[10] Mariani S, Ghisi A, Corigliano A, Zerbini S. Multi-scale analysis of MEMS sensors subject to drop impacts. Sensors 2007;7:1817–33.
[11] Mariani S, Ghisi A, Fachin F, Cacchione F, Corigliano A, Zerbini S. A three-scale FE approach to reliability analysis of MEMS sensors subject to drop impacts. Meccanica 2008;43:469–83.
[12] Hill R. The mathematical theory of plasticity. Oxford University Press; 1983. p. 19–23.
[13] Ardito R, Corigliano A, Frangi A. Modelling of spontaneous adhesion phenomena in micro-electro-mechanical systems. Eur J Mech – A/Solids 2013;39:144–52.
[14] Hu Y, Tonder K. Simulation of 3-D random surface by 2-D digital filter and Fourier analysis. Int J Machine Tools Manuf 1992;32:83–90.
[15] MIL-STD-883E. Test method standards for microcircuits. Department of Defense, USA; 1996 [method no. 2019].